Amino-functionalized mesostructured cellular foam silica: a highly efficient and recyclable catalyst in the Knoevenagel condensation reaction

Hao DONG, Hongyuan YANG, Tengfei ZHANG, Qing LIU*
Key Laboratory of Low Carbon Energy and Chemical Engineering,
College of Chemical and Environmental Engineering,
Shandong University of Science and Technology, Qingdao Shandong, P.R. China

Abstract: Mesostructured cellular foam silica was functionalized by an amino group (MCF-NH$_2$) using the postsynthesis grafting method and utilized as a recyclable catalyst for the Knoevenagel reaction to afford α, β-unsaturated compounds. The catalyst was systematically characterized by various analyses such as nitrogen adsorption, X-ray diffraction, Fourier transform infrared spectrophotometry, scanning electron microscopy, transmission electron microscopy, thermogravimetric analysis, and Hammett indicator method. The results showed that MCF-NH$_2$ catalyst was successfully prepared with a high surface area of 215 m^2 g^{-1} and a large pore volume of 1.37 cm^3 g^{-1}. Compared with the nonfunctionalized MCF sample, the window and cell sizes of MCF-NH$_2$ decreased after amino group modification, whose NH$_2$-loading density was 1.56 mmol g^{-1}. The optimal condition was investigated and the highest catalytic activity was obtained in the presence of 0.1 g of MCF-NH$_2$ catalyst under ultrasound irradiation at room temperature in the mixed solvent of ethanol and water with a volume ratio of 3:1. Various aromatic aldehydes and active methylene compounds were converted to their desired products with excellent yields within a short time. Moreover, MCF-NH$_2$ catalyst showed high recyclability, being used four times without any significant decrease in activity.

Key words: Mesostructured cellular foam silica, amino group, functionalization, recyclability, catalysis

1. Introduction

Mesostructured cellular foam (MCF) silica is a material with a 3-dimensional pore structure of large cells interconnected by narrower mesoporous pores[1] that has been utilized in many fields such as adsorption, separation, and catalysis because of its unique pore characteristics of high surface area and large pore volume.[2,3]

The surface of silica-based material can be modified with functional groups such as amine, mercapto, sulfonyl, and carboxyl. After functionalization, the related properties can be significantly enhanced for application in fields such as drug delivery, protein adsorption and desorption, and biomolecule loading.[4,5] Among them, amino-group functionalized mesoporous silica has been widely used to modify silica-based material surface because these groups are easily grafted to the silica surface at a high surface density.[5] Two major methods to modify the surface are direct cocondensation synthesis and postsynthesis grafting.[6] Compared with the direct cocondensation synthesis method, the postsynthesis grafting method is more facile and more easily controlled through the coupling reactions between surface silanol groups and (3-aminopropyl) triethoxysilane.[7]

The Knoevenagel condensation reaction is a well-known organic synthesis reaction to form the carbon–

---

*Correspondence: qliu@sdust.edu.cn

carbon bond that is usually carried out in the presence of basic catalysts. Following our research on catalysis and green synthesis,[8−12] amino-group functionalized MCF silica (MCF-NH$_2$) was prepared through the post-synthesis grafting method and utilized as the catalyst for this reaction. The reaction proceeded smoothly under mild conditions at room temperature under ultrasound irradiation with excellent yields within short times.

2. Experimental

2.1. Preparation of MCF

MCF was prepared using the method reported in the literature.[1] Pluronic 123 (4.0 g) was dissolved in HCl aqueous solution (150 mL, 1.6 M) at room temperature. After its complete dissolution, the mixture was heated to 40 °C, and then 1,3,5-trimethylbenzene (4.0 g), NH$_4$F (0.046 g), and tetraethylorthosilicate (8.8 g) were added under vigorous stirring. After further stirring for 20 h, the above mixture was transferred into an autoclave and heated at 130 °C for 24 h. Then the sample was collected by filtration, dried at room temperature, and calcined at 550 °C for 4 h with a heating rate of 1 °C min^{-1}.

2.2. Preparation of MCF-NH$_2$

The preparation of amino-functionalized MCF material was performed by the grafting method.[4] MCF (1.0 g, predried at 120 °C for 24 h) was introduced into anhydrous toluene (100 mL) containing (3-aminopropyl) triethoxysilane (3 mmol) in a flask (250 mL) at room temperature. After that, the mixture was heated to 80 °C in Ar flow for 6 h. Finally, MCF-NH$_2$ was collected by filtration and washed with toluene and anhydrous alcohol followed by drying at 60 °C for 24 h.

2.3. Characterizations

A surface area and pore size analyzer (Quantachrome, NOVA 3200e) was used to perform the N$_2$ adsorption analysis. The specific surface area was determined according to the Brunauer–Emmett–Teller (BET) method in the relative pressure range of 0.05–0.3. The window size was calculated with the Broekhoff–de Boer (BdB) method using the desorption isotherm branch and the cage size was calculated from the adsorption branch based on the BdB sphere model. A Nicolet 380 Fourier-Transform Infrared spectrophotometer (Thermo Electron Corporation, Waltham, MA, USA) was used to record the Fourier-transform infrared spectra (FT-IR) in the range of 400–4000 cm^{-1}. The Hammett indicator method was used to measure the basicity strength (H$_-$) of the MCF-NH$_2$ catalyst using bromothymol blue (H$_-$ = 7.2), phenolphthalein (H$_-$ = 9.8), and dinitroaniline (H$_-$ = 15.0) as Hammett indicators.[13] The total basicity number of the MCF-NH$_2$ catalyst was determined by volumetric titration using Hammett indicator–benzoic acid standard solution. A Rigaku Ultima IV X-ray diffraction (XRD) diffractometer (Rigaku Corporation, Osaka, Japan) was used to record the related patterns with a step of 0.02 using Cu K$_\alpha$ radiation (λ = 1.5418 Å) at 40 kV and 40 mA. An emission scanning electron microscope (SEM) (JSM-6700F, JEOL) and transmission electron microscope (TEM) (JEM-2010F, JEOL) were used to observe the morphology of the samples. A TGA 2 thermogravimetric analyzer was used to analyze the thermogravimetric (TG) analysis in air flow (200 mL min^{-1}) from room temperature up to 800 °C (10 °C min^{-1}). Melting points and ^{1}H NMR spectra were determined on a XT-4 micromelting point apparatus (Beijing Taike Instrument Company, China) and EFT-60 NMR spectrometer (Anasazi Instruments, New Palestine, IN, USA), respectively.

2.4. General procedure for Knoevenagel condensation

Typically, aromatic aldehyde (20 mmol) and active methylene compound (20 mmol) were mixed thoroughly in the presence of a certain solvent (4 mL) in a flask, and then the appropriate amount of MCF-NH$_2$ catalyst was added. The flask was then located at the maximum energy area in the ultrasonic cleaner to carry out the reaction at room temperature. After the completion of the reaction, the system was usually solidified. The mixture was then collected and dissolved in hot ethanol, and the catalyst was removed by filtration. After being washed with anhydrous ethanol, the recovered catalyst was able to be reused in the next reaction cycle. All the products were characterized by mp, IR, and ^{1}H NMR and are shown in the Supporting Information.

3. Results and discussion

3.1. Catalyst characterizations

3.1.1. BET

MCF and MCF-NH$_2$ materials were investigated by nitrogen adsorption analysis and the results are shown in Figure 1. The isotherm of MCF was type IV and showed steep hystereses of type H1 (Figure 1a).[14] In addition, the sharp rise at high relative pressures (P/P$_0$ above 0.8) indicated the existence of large mesopores and macropores in these materials.[1] After the amino-group functionalization, MCF-NH$_2$ showed an isotherm similar to that of MCF, indicating that its structure remained unchanged during the grafting process. As reported, MCF materials had ink-bottle-type pores in which large cells were interconnected by narrower windows.[15] BdB pore size analyses of the adsorption branches provided information about the cells (Figure 1b), whereas the desorption branches gave information regarding the windows (Figure 1c).[1] In Figure 1b, the cell size distribution curves of MCF and MCF-NH$_2$ are both highly narrow and the peaks of the curves are centered at around 41.6 and 35.1 nm, respectively. In addition, MCF and MCF-NH$_2$ showed similar window size curve distributions with peak values of 21.8 and 16.3 nm, respectively (Figure 1c). Obviously, the sizes of both cells and windows decreased after the silanization process, which provided further evidence of success amino-group functionalization over both the cells and windows of MCF material. As expected, the specific surface area and volume of MCF-NH$_2$ materials were significantly decreased due to the grafting of amino group over the pores of the MCF material (Table 1).

Table 1. Physical and chemical properties of the as-synthesized catalysts.

Sample	S_{BET} (m^2 g^{-1})^a	V_p (cm^3 g^{-1})^b	D_c (nm)^c	D$_w$ (nm)^d	NH$_2$-loading (mmol g^{-1})^e
MCF	343	1.97	41.6	21.8	–
MCF-NH$_2$	215	1.37	35.1	16.3	1.56

^{a}Surface area, derived from the BET equation.

^{b}Pore volume, obtained from the volume of nitrogen adsorbed at the relative pressure of 0.97.

^{c}Cell size, calculated from the adsorption branches of the N$_2$ adsorption isotherms based on the BdB sphere model.

^{d}D$_w$, window size, calculated from the desorption branches of the N$_2$ adsorption isotherms based on the BdB sphere model.

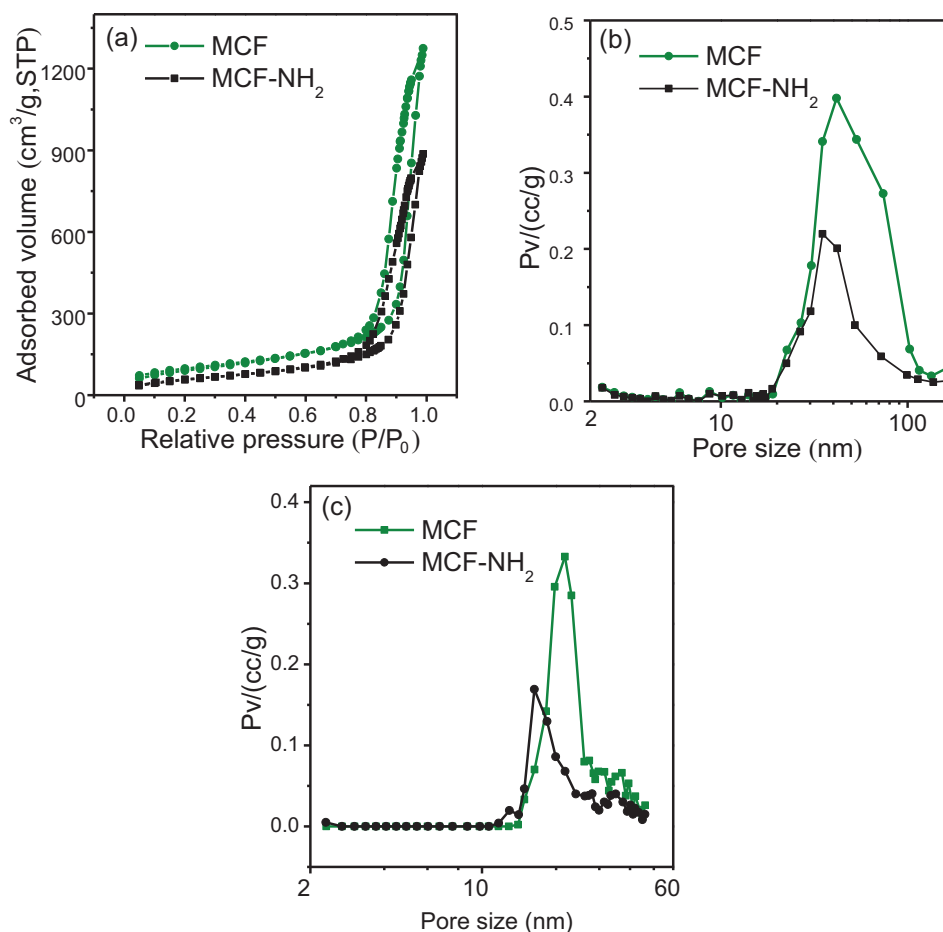^{e}NH$_2$ loading, derived from TGA results.

Figure 1. N_2 adsorption isotherms (a), BdB pore size distribution curves derived from desorption isotherm branch (b) and BdB pore size distribution curves derived from adsorption isotherm branch (c) of MCF and MCF-NH$_2$.

3.1.2. XRD

The small angle powder XRD patterns of MCF and MCF-NH$_2$ are shown in Figure 2a. It exhibited three characteristic peaks, indicating the presence of a mesoporous structure.[15] In addition, the intensities of each peak of MCF-NH$_2$ were similar to those of MCF, which suggested that its order degree of mesoporous structure did not change during the surface modification step. In addition, the wide-angle XRD patterns of MCF and MCF-NH$_2$ are shown in Figure 2b. Overall, similar XRD patterns with a wide diffraction peak at around 22.1° were observed, indicating the presence of an amorphous crystalline phase of silica over them.

3.1.3. FT-IR

In order to analyze the surface functional groups of MCF and MCF-NH$_2$ materials, the FT-IR spectra were recorded and are shown in Figure 3. Compared with MCF, the new band at around 693 cm^{-1} in the spectrum of MCF-NH$_2$ could be attributed to the presence of aminopropyl functionality with Si–C stretching vibration,[4] which provided evidence of the successful grafting of silane coupling agent on the surface of MCF. Moreover, the new broad bands at around 1470 and 1560 cm^{-1} could be assigned to the N–H bond of the amino group,[16,17] suggesting that the silane coupling agent had reacted with the hydroxyl groups of MCF. In a word, for MCF-
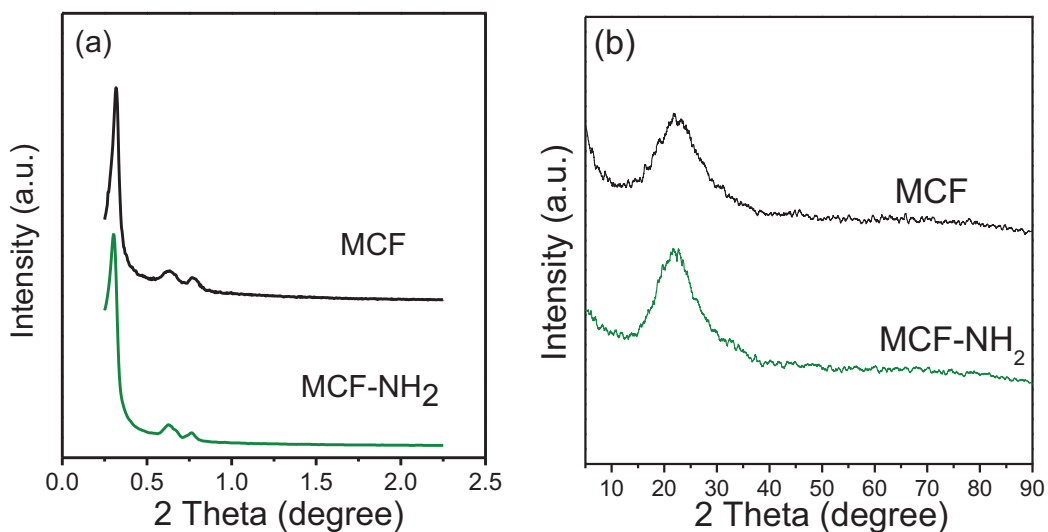
Figure 2. Small-angle XRD (a) and wide-angle XRD (b) patterns of MCF and MCF-NH$_2$.

NH$_2$, the amino group had been successfully grafted over the MCF framework using the postsynthesis grafting method.
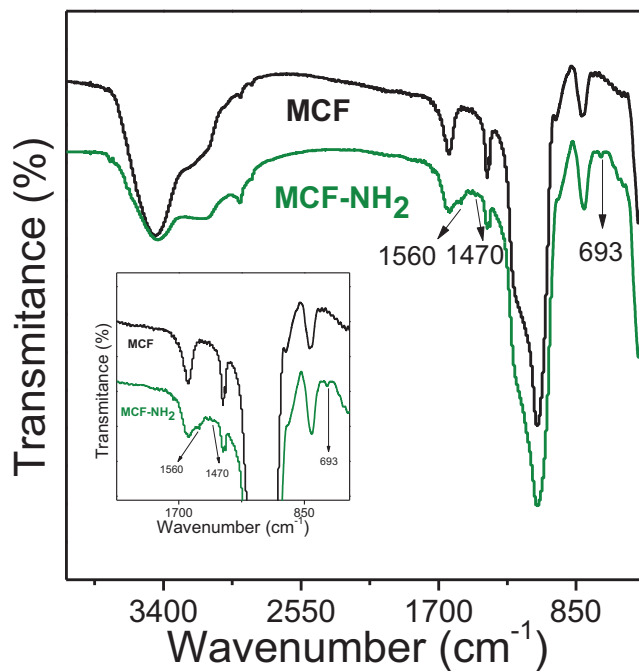

Figure 3. FT-IR spectra of MCF and MCF-NH$_2$.

3.1.4. SEM and TEM observations

SEM images of MCF and MCF-NH$_2$ are shown in Figure 4. After amino group functionalization, MCF-NH$_2$ material (Figures 4a and 4b) still retained the original morphology of MCF (Figures 4c and 4d) with many large external pores (foam), which facilitated the diffusion of substrates and products during the reaction process.
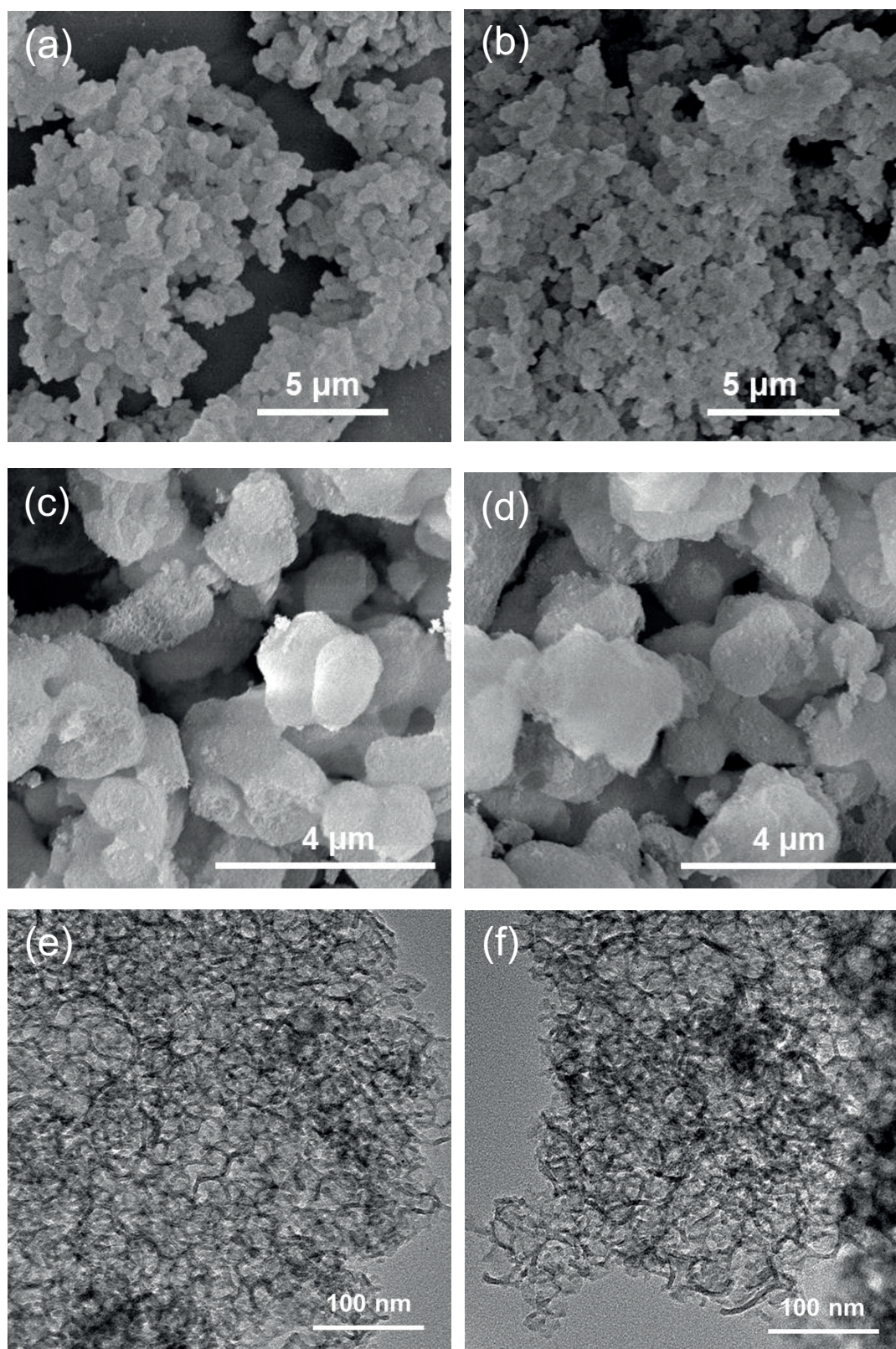
Figure 4. SEM images of MCF (a, b) and MCF-NH$_2$ (c, d); TEM images of MCF-12 (e) and MCF-NH$_2$ (f).

Figures 4e and 4f show the TEM images of MCF and MCF-NH$_2$ materials. Overall, the two samples exhibited similar morphology with a cell size of about 34 nm and a wall thickness of 3 to 4 nm.[5] The disordered mesoporous structure of the large spherical cells interconnected by windows was observed, which was the unique structural feature of the MCF. However, the amino group could not be observed in the TEM images due to its poor contrast.

3.1.5. TG analysis

In order to determine the density of the amino group over MCF-NH$_2$, TG analysis was conducted and the results are shown in Figure 5. For MCF, there was a weight loss peak at around 150 °C corresponding to the physically adsorbed water (Figure 5a). In addition, there was a weak weight loss peak at 433 °C due to partial decomposition of MCF with a total weight loss of 7.5 wt% (Figure 5a).[18] On the other hand, for MCF-NH$_2$, there were four weight loss peaks at around 199, 286, 379, and 466 °C, respectively (Figure 5b). Among them, the peaks at 379 and 466 °C were attributed to the decomposition of aminopropyl groups.[18] The total weight loss of MCF-NH$_2$ was 17.0%, which corresponded to the amino group with density of 1.56 mmol g^{-1} (Table 1).
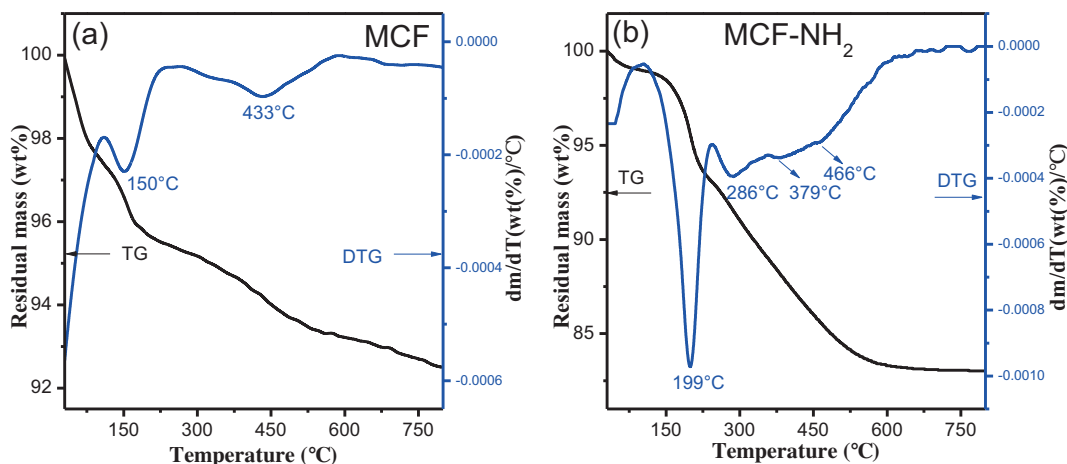

Figure 5. Thermogravimetric analysis of MCF (a) and MCF-NH$_2$ (b).

3.1.6. Hammett indicator method analysis

Basicity strength, total basicity number, and basicity concentration of the MCF-NH$_2$ catalyst are listed in Table 2, and MCF was also measured as the reference.[13,19] As seen, MCF exhibited weak basicity strength of H$_-$ < 7.2, and MCF-NH$_2$ showed higher basicity strength of 9.8 < H$_-$ < 15.0. Meanwhile, the total basicity number and basicity concentration of MCF-NH$_2$ were 2.3 mmol g^{-1} and 10.6 μmol m^{-2}, respectively. Compared with the amino group density (1.56 mmol g^{-1}) determined by TG, the total basicity number was similar, which provided further quantitative information of the amino group over the MCF-NH$_2$ material.

3.1.7. MCF-NH$_2$-catalyzed Knoevenagel reaction

3.1.8. Effect of solvent on the Knoevenagel reaction

The reaction of benzaldehyde and malononitrile was selected as the model reaction to optimize the reaction conditions. In order to investigate the solvent effect, various solvents were used for the model reaction in the
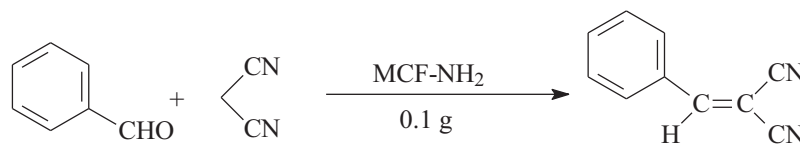
Table 2. Basicity strength, total basicity number, and basicity concentration measurement.

Sample	Basicity strength $(H_-)^a$	Total basicity number $(mmol\ g^{-1})^a$	Basicity concentration $(\mu mol\ m^{-2})^b$
MCF	< 7.2	–	–
MCF-NH$_2$	9.8 < H$_-$ < 15	2.3	10.6

[a]Measured by the Hammett indicators method.

[b]Basicity concentration = Total basicity number/specific surface area.

presence of MCF-NH$_2$ at room temperature (Table 3). This reaction solidified completely in 25.0 min under solvent-free conditions using the magnetic stirring method with a yield of 82%. However, when the reaction was performed under ultrasound irradiation, the time decreased to 22.0 min with a higher yield of 90%. Obviously, the ultrasound-assisted method was more efficient than the magnetic stirring method for this reaction;[8] thus, the ultrasound-assisted method was used in the subsequent reactions.

Table 3. Effect of solvent on Knoevenagel condensation of benzaldehyde with malononitrile.[a]

Entry	Catalyst	Solvent	Time (min)	Yield (%)^b
1	MCF-NH$_2$	Solvent-free^c	25.0	82
2	MCF-NH$_2$	Solvent-free^d	22.0	90
3	MCF-NH$_2$	C$_2$H$_5$OH^d	36.0	91
4	MCF-NH$_2$	H$_2$O^d	8.7	88
5	MCF-NH$_2$	C$_2$H$_5$OH-H$_2$O (3:1)^{d,e}	1.0	94
6	MCF-NH$_2$	C$_2$H$_5$OH-H$_2$O (2:2)^{d,e}	2.7	92
7	MCF-NH$_2$	C$_2$H$_5$OH-H$_2$O (1:3)^{d,e}	3.5	93
8	Catalyst-free	Solvent-free^c	660.0	trace
9	MCF	Solvent-free^c	660.0	trace

[a]Reaction conditions: benzaldehyde (20 mmol), malononitrile (20 mmol), solvent (4 mL), room temperature.

[b]Isolated yield.

[c]Magnetic stirring.

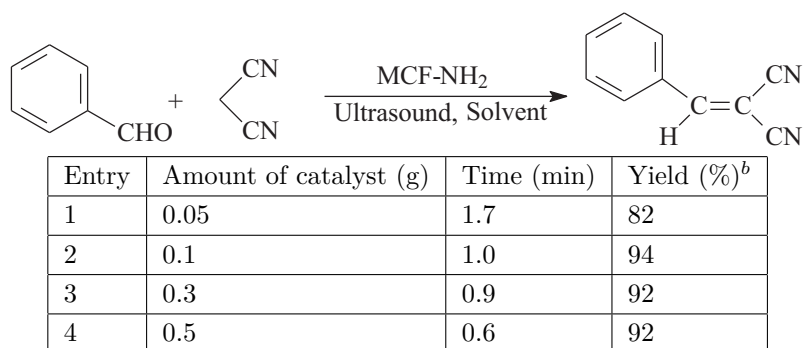[d]Ultrasound irradiation.

[e]Volume ratio.

In addition, ethanol and water were investigated as the solvent. Compared with the solvent-free reaction, ethanol was adverse for this reaction with a longer reaction time. Meanwhile, H$_2$O enhanced the reaction and the reaction finished in 8.7 min with a yield of 88%. To our surprise, the mixed solvents of H$_2$O and ethanol seemed to be more efficient for this reaction, and it finished in only 1.0 min with a yield of 94% in a mixture of ethanol and H$_2$O (3:1, volume ratio). In order to highlight the improvement of solvent effect, the model reaction was also investigated in the presence of MCF or without catalyst under solvent-free conditions (entries 8 and 9). The yields were trace after the reaction time of 11 h, indicating that the Knoevenagel reaction could not

be performed in the presence of MCF or without catalyst under solvent conditions. As we all knew, H_2O and ethanol were two typical environmentally friendly solvents crucial for organic synthesis reactions.[20] Therefore, considering the environment-friendly property of both water and ethanol, the mixed solvent of ethanol and water (3:1) was used as the solvent in the following experiments.

3.1.9. Effect of amount of catalyst

The optimal amount of MCF-NH$_2$ was investigated for the model reaction. In the above experiments, 0.1 g catalyst was used and the yield of the model reaction was 94% under ultrasound irradiation at room temperature in the mixed solvent of ethanol and water. When the amount of catalyst was reduced to 0.05 g, the reaction time was prolonged to 1.7 min with a yield of only 82% (Table 4, entry 1). Therefore, more catalyst was added, and the reaction time was reduced to below 1 min with a yield around 92%. Considering the above results, the optimal amount of MCF-NH$_2$ is 0.1 g in this work.

Table 4. Effect of catalyst amount on Knoevenagel condensation of benzaldehyde with malononitrile.[a]

Entry	Amount of catalyst (g)	Time (min)	Yield (%)[b]
1	0.05	1.7	82
2	0.1	1.0	94
3	0.3	0.9	92
4	0.5	0.6	92

[a]Reaction conditions: benzaldehyde (20 mmol), malononitrile (20 mmol) under ultrasound irradiation in a mixture of ethanol and H_2O (3:1) at room temperature;
[b]Isolated yield.

3.1.10. Universality of MCF-NH$_2$ for Knoevenagel condensation

In order to investigate the universality of MCF-NH$_2$ catalyst for the Knoevenagel reaction with various aromatic aldehydes and active methylene compounds, eight different substrates were used in the presence of 0.1 g of MCF-NH$_2$ and the results are shown in Table 5. Overall, the aldehydes containing both electron-withdrawing and electron-donating groups could react with malononitrile and ethyl cyanoacetate to afford the corresponding products in short times with high yields. In particular, the reaction of 4-chlorobenzaldehyde and malononitrile solidified in 0.2 min with a yield of 87%. Furthermore, compared with malononitrile, ethyl cyanoacetate showed much lower activity due to the poor electron-withdrawing ability of the ester group, which is reported in the literature.[21,22]

In addition, MCF-NH$_2$ catalyst could be used four times without a significant decrease in reactivity, indicating its high reusability in this work (Table 6). As seen in the FT-IR spectra in Figure 6, the functional groups of the recovered MCF-NH$_2$ catalyst at 693, 1470, and 1560 cm^{-1} remained unchanged after each cycle, indicating that MCF-NH$_2$ was a highly recyclable catalyst for the Knoevenagel reaction.

Table 5. Knoevenagel condensation catalyzed by MCF-NH$_2$ using an ultrasound-assisted method.[a]

$$RCHO \quad + \quad H_2C \overset{CN}{\underset{X}{<}} \quad \xrightarrow[\text{Ultrasound,Slovent}]{MCF-NH_2} \quad \overset{R}{\underset{H}{>}}C=C\overset{CN}{\underset{X}{<}}$$
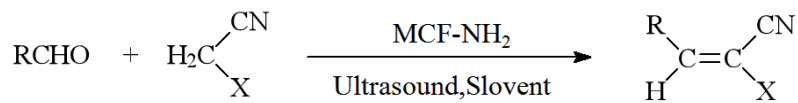
Entry	R	X	Time (min)	Yield (%)[b]
1	C$_6$H$_5$	CN	1.0	94
2	4-ClC$_6$H$_4$	CN	0.2	87
3	4-CH$_3$C$_6$H$_4$	CN	2.2	96
4	4-CH$_3$OC$_6$H$_4$	CN	1.3	92
5	Vanillin	CN	6.0	90
6	2-Furyl	CN	2.5	91
7	4-ClC$_6$H$_4$	COOEt	31.3	89
8	4-CH$_3$C$_6$H$_4$	COOEt	45.0	90

[a]Reaction conditions: benzaldehyde (20 mmol), the active methylene compound (20 mmol), 0.1 g of MCF-NH$_2$, in a mixture of ethanol and H$_2$O (3:1) with ultrasound irradiation at room temperature.
[b]Isolated yield.

Table 6. The reusability of MCF-NH$_2$ for the Knoevenagel reaction.[a]

Cycle	1	2	3	4
Time (min)	1.0	1.7	1.2	1.5
Yield (%)[b]	94	89	92	91

[a]Reaction conditions: benzaldehyde (20 mmol), malononitrile (20 mmol), MCF-NH$_2$ (0.1 g), ultrasound irradiation, ethanol, and H$_2$O (3:1, total 4 mL), room temperature.
[b]Isolated yield.
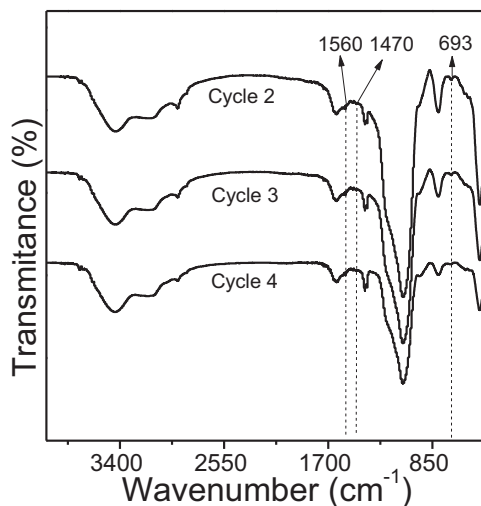
Figure 6. FT-IR spectra of MCF-NH$_2$ in the reusability test.

3.2. Conclusions

Amino-group functionalized mesostructured cellular foam silica (MCF-NH$_2$) material was prepared by a post-synthesis grafting method and utilized as the catalyst for the Knoevenagel reaction in this work. After amino group functionalization, the NH$_2$-loading density was as high as 1.56 mmol g^{-1} determined by TGA, which was crucial for the basic catalyzed Knoevenagel reaction. The reaction conditions were optimized and the highest catalytic activity was obtained in the presence of 0.1 g of MCF-NH$_2$ catalyst under ultrasound irradiation at room temperature in the mixed solvent of ethanol and water with a volume ratio of 3:1. Various substrates afforded the corresponding products with high yields in short reaction times under the optimal conditions. MCF-NH$_2$ could be used four times without a significant decrease in reactivity. The attractive features of this procedure were the mild reaction conditions, high yields, recyclability, environmentally friendly reaction profiles, and operational simplicity.

References

1. Kim, J.; Desch, R. J.; Thiel, S. W.; Guliants, V. V.; Pinto, N. G. *Microporous Mesoporous Mater.* **2012**, *149*, 60-68.

2. Szymańska, K.; Bryjak, J.; Mrowiec-Białoń, J.; Jarzębski, A. B. *Microporous Mesoporous Mater.* **2007**, *99*, 167-175.

3. Subagyono, D. J. N.; Marshall, M.; Knowles, G. P.; Chaffee, A. L. *Microporous Mesoporous Mater.* **2014**, *186*, 84-93.

4. Xu, S.; Yong, J.; Lai, G.; Zhang, H.; Wu, Y.; Yu, A. *Chem. Lett.* **2013**, *42*, 235-237.

5. Yan, X.; Zhang, L.; Zhang, Y.; Qiao, K.; Yan, Z.; Komarneni, S. *Chem. Eng. J.* **2011**, *168*, 918-924.

6. Sujandi, E. A.; Park, S. E. *Appl. Catal. A Gen.* **2008**, *350*, 244-251.

7. Sanz, R.; Calleja, G.; Arencibia, A.; Sanz-Pérez, E. S. *Microporous Mesoporous Mater.* **2012**, *158*, 309-317.

8. Liu, Q.; Ai, H.; Li, Z. *Ultrason. Sonochem.* **2011**, *18*, 477-479.

9. Yang, H.; Dong, H.; Zhang, T.; Zhang, Q.; Zhang, G.; Wang, P.; Liu, Q. *Catal. Lett.* **2019**, *149*, 778 787.

10. Liu, Q.; Ai, H. *Synth. Commun.* **2012**, *42*, 3004-3010.

11. Dong, H.; Liu, Q.; Tian, Y.; Qiao, Y. *J. Chem. Res.* **2018**, *42*, 463-466.

12. Liu, Q.; Ai, H.; Feng, S. *Synth. Commun.* **2012**, *42*, 122-127.

13. Algoufi, Y. T.; Kabir, G.; Hameed, B. H. *J. Taiwan Inst. Chem. Eng.* **2017**, *70*, 179-187.

14. Bocanegra, S. A.; Ballarini, A. D.; Scelza, O. A.; de Miguel, S. R. *Mater. Chem. Phys.* **2008**, *111*, 534-541.

15. Schmidt-Winkel, P.; Lukens, W. W.; Yang, P.; Margolese, D. I.; Lettow, J. S.; Ying, J. Y.; Stucky, G. D. *Chem. Mater.* **2000**, *12*, 686-696.

16. Heidari, A.; Younesi, H.; Mehraban, Z. *Chem. Eng. J.* **2009**, *153*, 70-79.

17. Fellenz, N.; Perez-Alonso, F. J.; Martin, P. P.; García-Fierro, J. L.; Bengoa, J. F.; Marchetti, S. G.; Rojas, S. *Microporous Mesoporous Mater.* **2017**, *239*, 138-146.

18. Saravanamurugan, S.; Sujandi; Han, D. S.; Koo, J. B.; Park, S. E. *Catal. Commun.* **2008**, *9*, 158-163.

19. Ilgen, O. *Fuel Process. Technol.* **2011**, *92*, 452-455.

20. Shuai, L.; Luterbacher, J. *ChemSusChem* **2016**, *9*, 133-155.

21. Wang, X. S.; Zeng, Z. S.; Li, Y. L.; Shi, D. Q.; Tu, S. J.; Wei, X. Y.; Zong, Z. M. *Synth. Commun.* **2005**, *35*, 1915-1920.

22. Rong, L.; Li, X.; Wang, H.; Shi, D.; Tu, S.; Zhuang, Q. *Synth. Commun.* **2006**, *36*, 2407-2412.

Supporting Information

Amino-functionalized mesostructured cellular foam silica: A highly efficient and recyclable catalyst in Knoevenagel condensation reaction

Hao DONG, Hongyuan YANG, Tengfei ZHANG, Qing LIU*

Key Laboratory of Low Carbon Energy and Chemical Engineering, College of Chemical and Environmental Engineering, Shandong University of Science and Technology, Qingdao Shandong 266590, China

*Corresponding author. E-mail address: qliu@sdust.edu.cn (Q. Liu)

Analytical Data for All the Compounds

2-(Phenylmethylene)malononitrile (Compound 1).

Mp 82–83 $^{\circ}$C, ^{1}H NMR (CDCl$_3$) δ: 7.56 (t, 2H, J = 7.5 Hz, Ar-H), 7.68 (t, 1H, J = 7.5 Hz, Ar-H), 7.81 (s, 1H, CH=C), 7.95 (d, 2H, J = 7.6 Hz, Ar-H); IR (KBr) v (cm^{-1}): 2222, 1659, 1595, 1563, 1435, 1217.

2-(4-Chlorophenylmethylene)malononitrile (Compound 2).

Mp 159–161 $^{\circ}$C, ^{1}H NMR (CDCl$_3$) δ: 6.96–7.29 (d, 2H, J = 8.3 Hz, Ar-H), 7.50 (d, 2H, J = 8.3 Hz, Ar-H), 7.61 (s, 1H, C=CH); IR (KBr) v (cm^{-1}): 3748, 3672, 3097, 3033, 2225, 1584.

2-(4-Methoxyphenylmethylene)malononitrile (Compound 3).

Mp 111–113 $^{\circ}$C, ^{1}H NMR (CDCl$_3$) δ: 3.94 (s, 3H, CH$_3$), 7.05 (d, J = 9.2 Hz, 2H, Ar-H), 7.68 (s, 1H, CH=C), 7.93 (d, J = 9.2 Hz, 2H, Ar-H); IR (KBr) v (cm^{-1}): 2211, 1598, 1559, 1509, 1365, 1190.

2-(4-MethylPhenylmethylene)malononitrile (Compound 4).

Mp 132–134 $^{\circ}$C, ^{1}H NMR (CDCl$_3$) δ: 0.21 (s, 3H, CH$_3$), 5.15 (d, J=8.4Hz, 4H, Ar-H), 5.64 (s, 1H, CH=C); IR (KBr) v (cm^{-1}): 3748, 3672, 3097, 2225, 1584, 1093.

2-[(4-Hydroxy-3-methoxyphenyl)methylene]malononitrile (Compound 5).

Mp 133–135 ^{o}C, ^{1}H NMR (CDCl$_3$) δ: 4.00 (s, 3H, CH$_3$O), 6.36 (s, 1H, OH), 7.06 (d, J = 8.4 Hz, 1H, Ar-H), 7.34 (d, J = 8.4 Hz, 1H, Ar-H), 7.65 (s, 1H, Ar-H), 7.76 (s, 1H, CH=C); IR (KBr) v (cm^{-1}): 2228, 1603, 1563, 1519, 1463, 1192.

2-(2-Furylmethylene)malononitrile (Compound 6).

Mp 65–66 ^{o}C, ^{1}H NMR (CDCl$_3$) δ: 6.74-6.75 (m, 1H, furfuryl), 7.39 (m, 1H, furfuryl), 7.54 (s, 1H, CH=C), 7.84 (s, 1H, furfuryl); IR (KBr) v (cm^{-1}): 3124, 3047, 2236, 1743, 1532, 1295.

Ethyl (*E*)-3-(4-chlorophenyl)-2-cyano-2-propenoate (Compound 7).

Mp 86–87 ^{o}C, ^{1}H NMR (CDCl$_3$) δ: 0.86–1.09 (t, 3H, J =7.1 Hz, CH$_3$), 3.91–4.15 (q, 2H, J = 7.2 Hz, CH$_2$), 7.48 (d, 2H, J =8.4 Hz, Ar-H), 7.55 (d, 2H, J=8.4 Hz, Ar-H), 7.83 (s, 1H, CH=C); IR (KBr) v (cm^{-1}): 3432, 2989, 2222, 1918, 1723, 1202.

Ethyl (*E*)-2-cyano-3-(4-Methylphenyl)-2-propenoate (Compound 8).

Mp 91–93 ^{o}C, ^{1}H NMR (CDCl$_3$) δ: 0.98–1.20 (t, 3H, J =7.1 Hz, CH$_3$), 2.14 (t, 3H, J =7.1 Hz, CH$_3$), 3.91–4.15 (q, 2H, J = 7.2 Hz, CH$_2$), 7.07 (d, 2H, J

=8.4 Hz, Ar-H), 7.54 (d, 2H, J=8.4 Hz, Ar-H), 7.92 (s, 1H, CH=C); IR

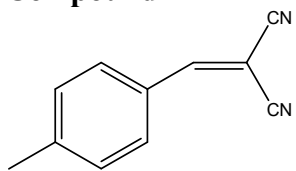(KBr) v (cm^{-1}): 3430, 2994, 2216, 1722, 1271, 1187.

Compound 1

Compound 2

3051.55
2220.52
1653.23
1583.56
1464.13
1439.25
1369.58
1284.98
1205.36
1125.74
1046.12
961.53
757.50
697.79
618.17
463.90

Compound 3

IR spectrum peaks (cm⁻¹):
3808.50, 3034.43, 2957.67, 2234.83, 2220.51, 1932.48, 1873.98, 1625.80, 1615.71, 1605.42, 1585.79, 1553.49, 1506.79, 1449.01, 1411.60, 1370.63, 1298.88, 1218.27, 1201.47, 1187.74, 1146.60, 1038.40, 959.25, 938.58, 813.77, 757.53, 707.03, 613.79, 564.15, 515.69
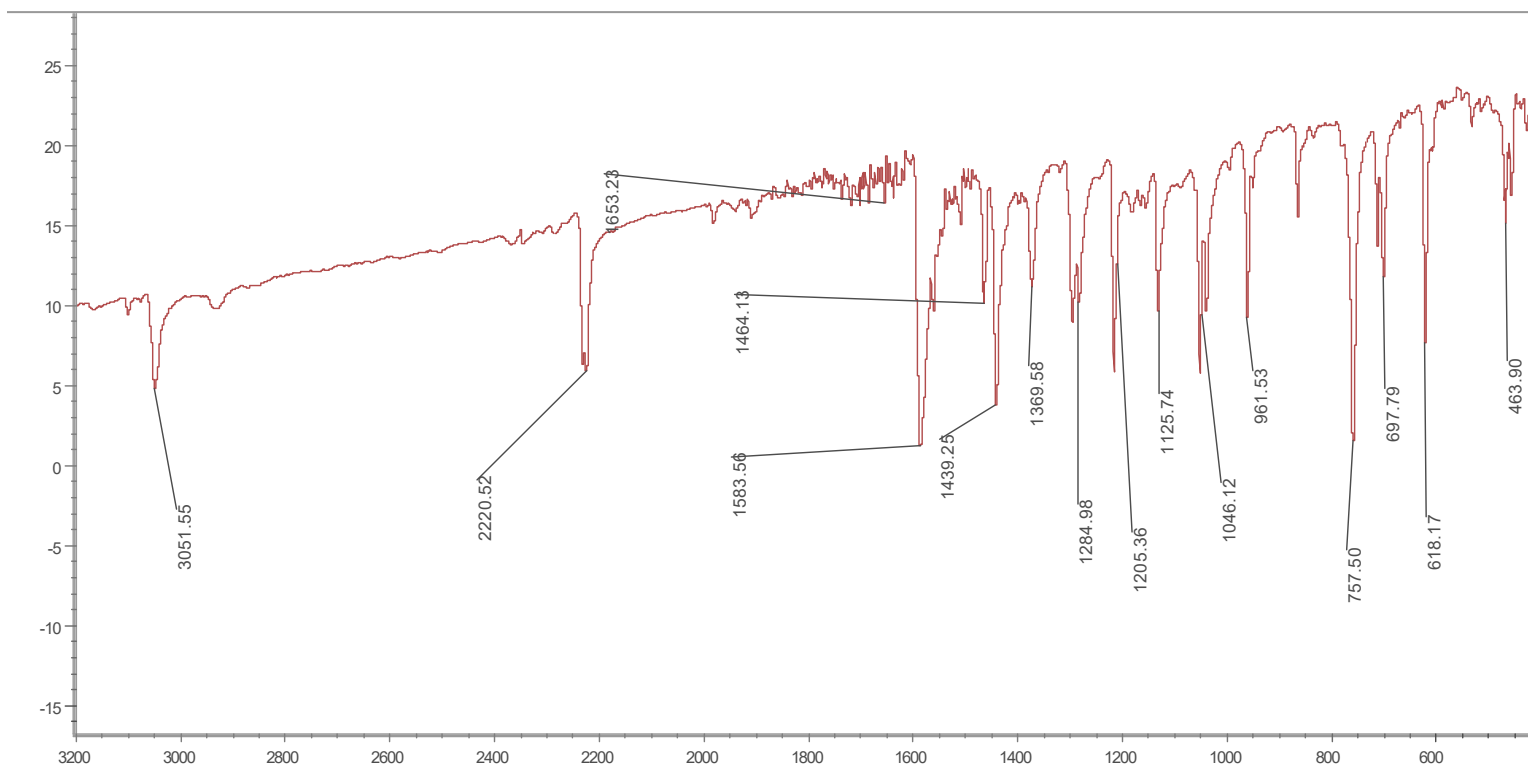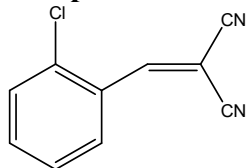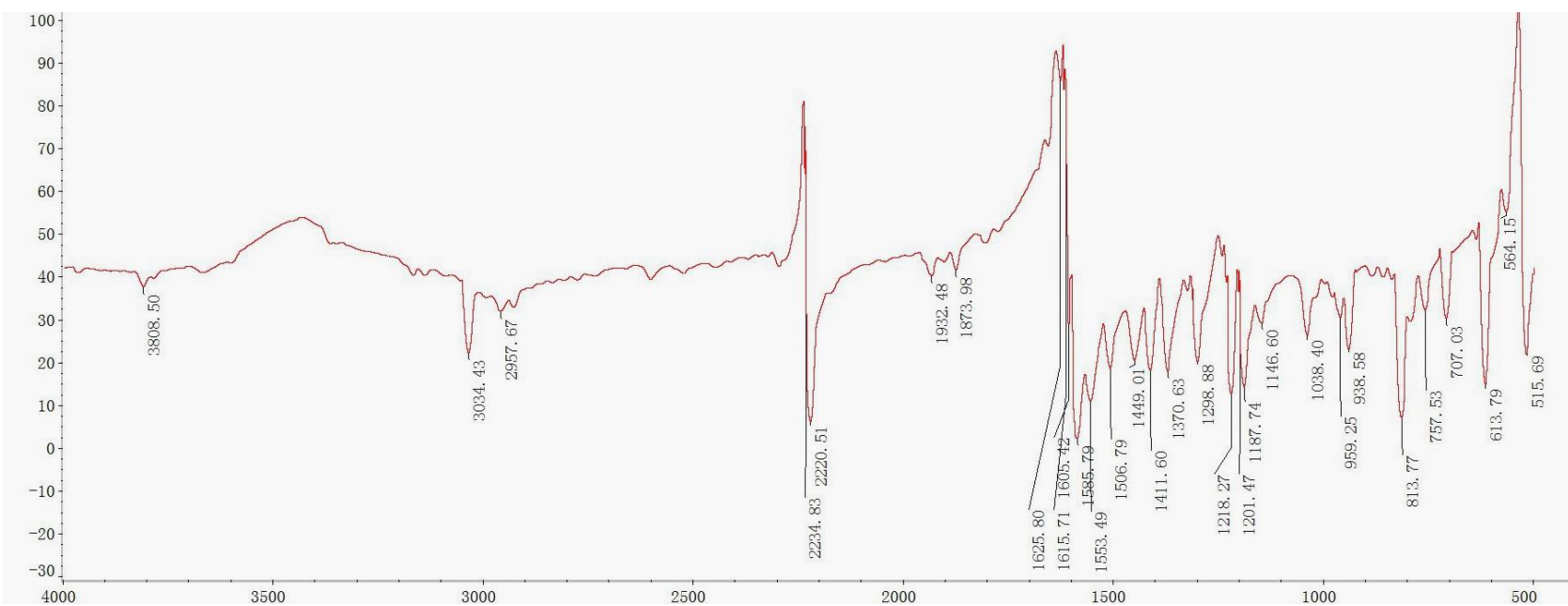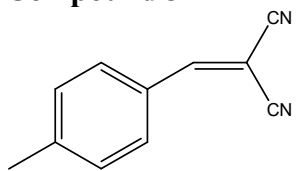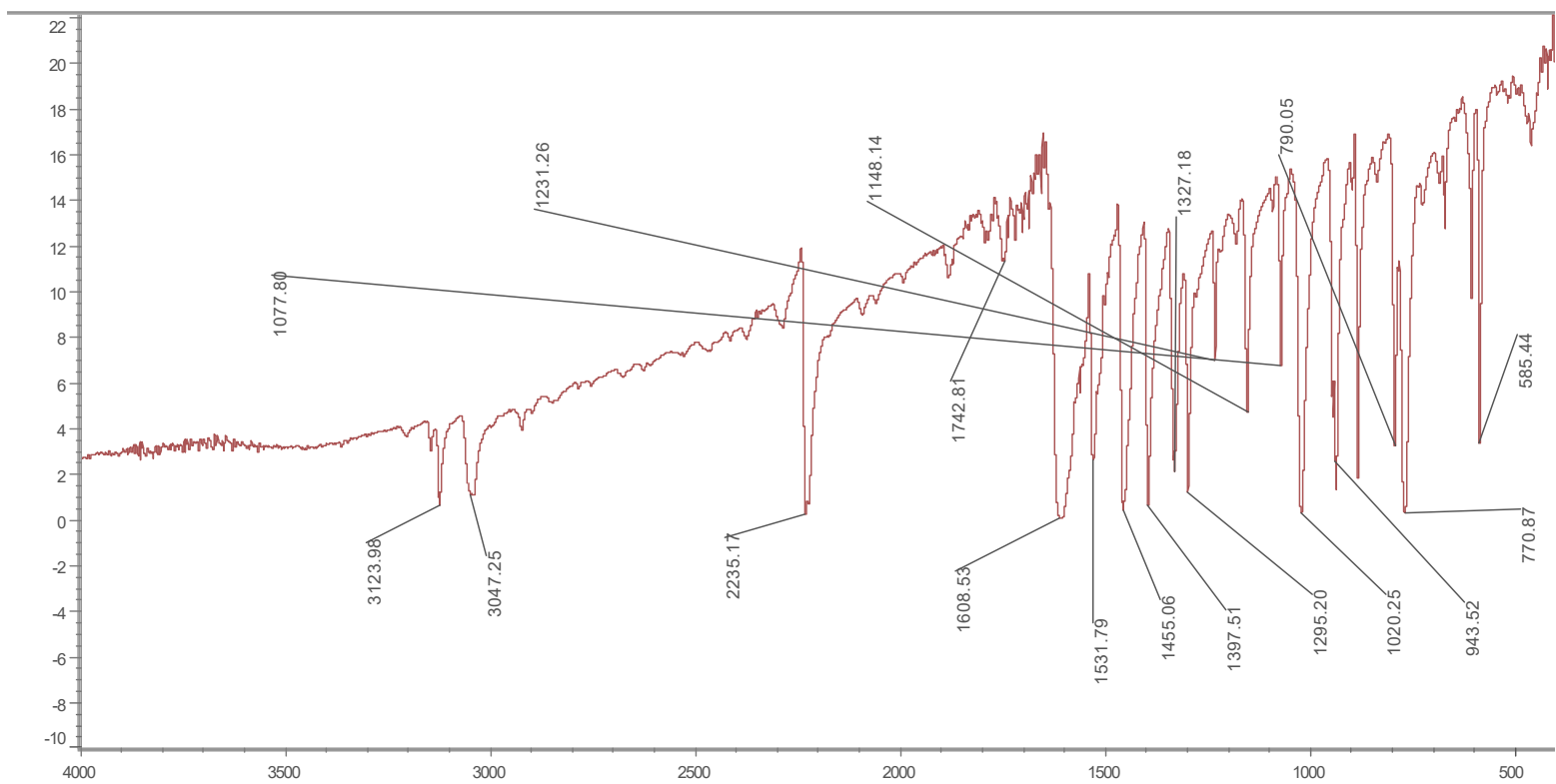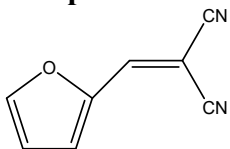
Compound 4

Compound 5

Compound 6

**Y2

Peak label
3432.28
3036.89
2989.35
2952.48
2901.02
2370.57
2222.10
1957.41
1917.71
1723.21
1611.96
1588.29
1491.98
1447.75
1410.05
1363.56
1310.78
1264.52
1202.36
1079.45
1011.66
980.52
895.94
857.11
830.20
795.26
758.07
707.03
660.34
581.91
537.31

Compound 7

Compound 8

**S1

Peaks: 3429.54, 2993.69, 2215.78, 1826.23, 1722.39, 1640.56, 1596.35, 1512.65, 1453.24, 1397.36, 1366.64, 1271.33, 1210.77, 1186.50, 1124.69, 1089.38, 1017.59, 894.39, 849.58, 815.48, 759.53, 710.77, 585.73, 542.65

Compound 1

7.947
7.932
7.810
7.680
7.665
7.650
7.589
7.573
7.558

2.11
1.00
1.02
2.09

8.00
7.50

Compound 2

Compound 3

5.636
5.503
5.010

0.207

0.53
4.00

2.43

Compound 4

7.950
7.933
7.682
7.287
7.284
7.049
7.032

3.943

200

150

100

50

0

2.09
1.00
2.08
3.35

8.0
7.0
6.0
5.0
4.0

Compound 5

Compound_6

7.835
7.832
7.538
7.393
7.386
7.285
6.748
6.745
6.741
6.738

1.05   1.00   1.04   1.05

7.50   7.00

Compound 7

Compound 8